LUMiReader X-Ray: A New Instrument to Analyse Separation Behaviour of both Transparent and Opaque Concentrated Dispersions

D. Lerche*,**, D. Kavianpour**, A. Zierau* and T. Sobisch*
*LUM GmbH, **Dr. Lerche KG
Justus-von-Liebig-Str. 3 12489 Berlin/Germany info@lum-gmbh.de;
www.lum-gmbh.com

ABSTRACT

Detailed evaluation of the separation behaviour of dispersions is problematic for concentrated dispersions, even more, if the dispersed phase is a mixture of two or more materials. It is difficult to define a separation level or to trace differences in solids concentration over the entire sample by optical methods. For these tasks the LUMiReader® X-Ray has been developed, extending the STEP-Technology® (Space and Time resolved Extinction Profiles) to much shorter wavelength of X-rays. The new measuring principle allows qualitative and quantitative characterization of dispersion state of entire samples even in case of highly concentrated formulations and products independent on its optical properties – transparent or opaque. Experimental analysis is performed in situ (contact-free) with nascent, undiluted samples. The developed analyser can quantify the homogeneity of a dispersed phase (dispersibility) and determine concentration profiles in dispersions, sediments, and filter cakes. Latter is of great importance for separation unit processes like filtration, settling and centrifugation. Even more, information may be obtained regarding structure and mechanical properties of sediments, nature of particle-particle interactions as well as degree of flocculation. Importantly, for binary suspensions (mixtures of different dispersed materials), segregation can be evaluated based on different X-ray absorption of dispersed particles. Recently it was shown that nanoparticles may be detected in transparent supernatants as well as after phase separation in a highly opaque cosmetic matrix. This is increasingly important for nanodispersions, which are often transparent even for high volume concentration due to small Rayleigh-scattering. This paper describes the working principle of LUMiReader X-Ray and validation of measuring principle. Its applicability is demonstrated regarding separation kinetics, packing and concentration profiles of sediments as well as segregation phenomena of micro- and nano-dispersions.

Keywords

Cake Structure, Clarification, Concentration Profile, Nanoparticles, Solid-Liquid Separation, Sediment Compressibility, Segregation, X-ray,

INTRODUCTION

More and more products in industry as well as at consumer market are based on concentrated dispersions (suspensions, emulsions). Practically all food products, cosmetics, paints, pharmaceuticals can be described as such. On the other hand, high concentrated dispersions are essential for development of innovative energy storage means or fuel cells, to name a few technological challenges. Proper characterization of these systems would be important for new and optimization of formulation and

quality control of their later processing. For a long time there has been very limited set of methods and tools available for characterizing these systems in their nascent state. Most methods that have been used for this purpose required dilution. Such dilution affects system properties. For example, information regarding the stability of a dispersion formulation, sedimentation and creaming, disperse phase interaction (e.g. flocculation, agglomeration, aggregation, coalescence) and its change during the life span of the product can only be reliable studied on the formulation in its original undiluted state.

On the other hand, traditional methods employ “one point” measurement, means information is obtained only for a little volume of total sample. Recent technical ISOReport ISO/TR 13097 [1] demands therefore methods with space resolution to analyze the entire sample.

Patented space and time resolved extinction profiling (STEP-Technology) was successfully applied to characterize dispersion state for wide range of formulations and products [2, 3]. Traditional NIR-wavelength sources were used to avoid complications due to absorption of continuous or dispersed phase. To increase sensitivity to nanoparticle sizes down to some tens of nanometers, recently LUMiReader and LUMiSizer were equipped with additional blue wavelength sources [4]. High concentrated nascent dispersions may be analyzed by decreasing optical path correspondingly [5].

Another convenient approach to analyze high concentrated dispersions would be the use of X-ray radiation sources. X-rays transmit materials more efficiently compared to electromagnetic waves of longer wavelengths as visible light. An additional advantage is that, in contrast to light, transmitted intensity does not depend nether on shape or on size of dispersed particles.

The paper describes the working principle of LUMiReader X-Ray and its validation. Applications are highlighted regarding separation kinetics, packing and concentration profiles of sediments as well as segregation phenomena of micro- and nanodispersions.

BASIC PRINCIPLES OF STEP-TECHNOLOGY X-RAY

In contrast to traditional STEP-Technology® an X-ray tube with a molybdenum anode combined with a special anisotropic crystal generates parallel quasi monoenergetic Xray radiation which transmits the sample to be analysed (range of interest > 20 mm). Samples to be analysed are filled in 2 mm or 10 mm polycarbonate or polyamide cells (general one-way accessories for optical LUMiReader or LUMiSizer) and placed into the analyser. Sample volume are 0.4 ml or 1.6 ml. Transmitted intensities at programmable time intervals t_i are recorded by means of a special line sensor and space resolved intensity profiles $I(x,t_i)$ are digitized, displayed and stored at PC (cp. Fig. 1). Sampling time for a given profile amounts 300 ms. Measurement time of intensity profiles are colour coded (red profile at beginning (t_0) and dark green at the end (t_{end}). Temporal intensity changes represent rate of concentration changes of continuous or dispersed phase within the dispersion sample during observation time e.g., due to sedimentation or creaming. As depicted in Fig. 2, experimentally determined transmitted intensity I_{sample} for each spatial position and measurement time can be converted based on Lambert-Beer law into attenuation μ_{exp}, where I_0

corresponds to incident X-ray intensity and *d* to geometrical path. For clarity we dropped indices for position and time.

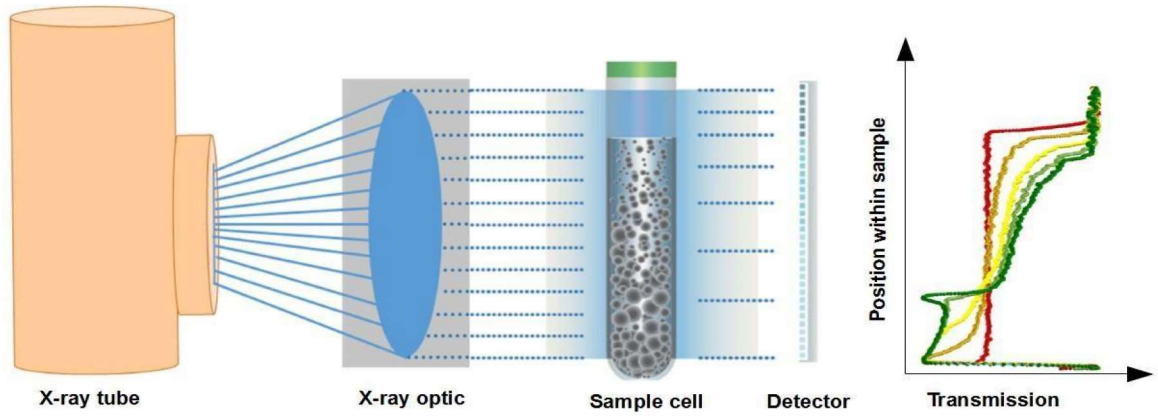

FIGURE 1: Measuring principle of LUMiReader X-Ray. Changes of particle concentration during phase separation are characterized by transmission profiles at programmable time intervals (right picture; red profile at beginning (t_0) and dark green at t_{end}.

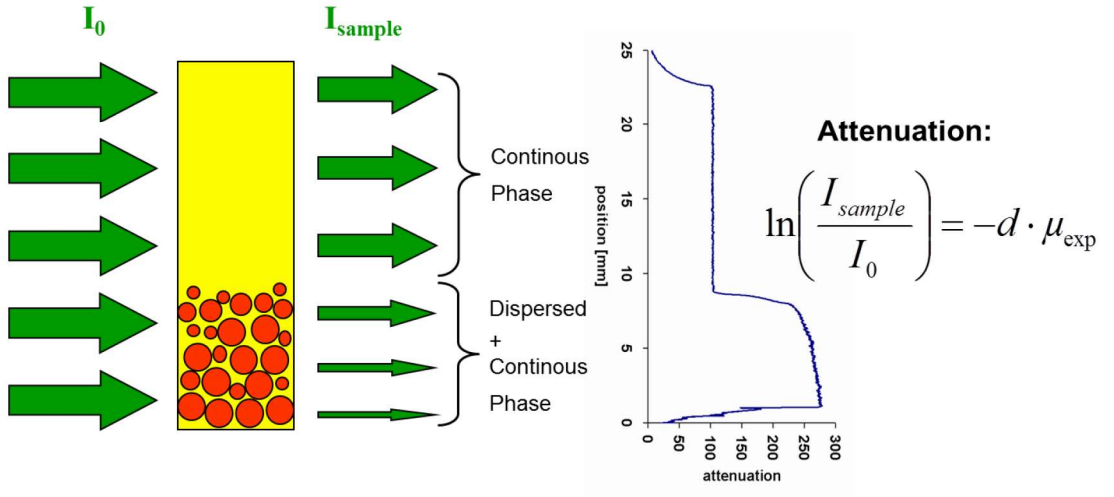

FIGURE 2: General approach to determine volume concentration of phases within a dispersion (sediment) based on experimentally determined mass attenuation μ_{exp} (details see below).

Volume concentration, e.g., of dispersed phase (α_{disp}), is calculated according to the equation below, where μ_{con} and μ_{disp} are the linear mass attenuation coefficients of pure continuous phase and dispersed material, respectively.

$$\alpha_{disp} = \frac{\mu_{\exp} - \mu_{con}}{\mu_{disp} - \mu_{con}}$$

X-ray mass attenuation coefficients depend on the atomic number(s) of materials and incident energy of photons. Therefore, a monoenergetic (monochrome) incident radiation is of great importance. Monochromaticity amounts 95.51 % ($K_{\square}$-line) of total incident radiation energy spectrum for above described instrumental setup. Very

important to underline furthermore that X-ray mass attenuation coefficients are not dependent neither on size nor shape of dispersed particles. This is a major advantage compared to any optical method. On the other hand, X-rays penetrate much higher volume concentrations and multiple scattering is mostly avoided.

Contrast or spatial resolution was verified by physical standards. On the one hand a stair like block with steps of 1 mm height and depths of 2 mm, manufactured from high purity graphite, was used to test contrast sensitivity. It was positioned instead of a sample cell and transmission recorded. As Fig. 3 shows, changes of material thickness were recorded adequately.

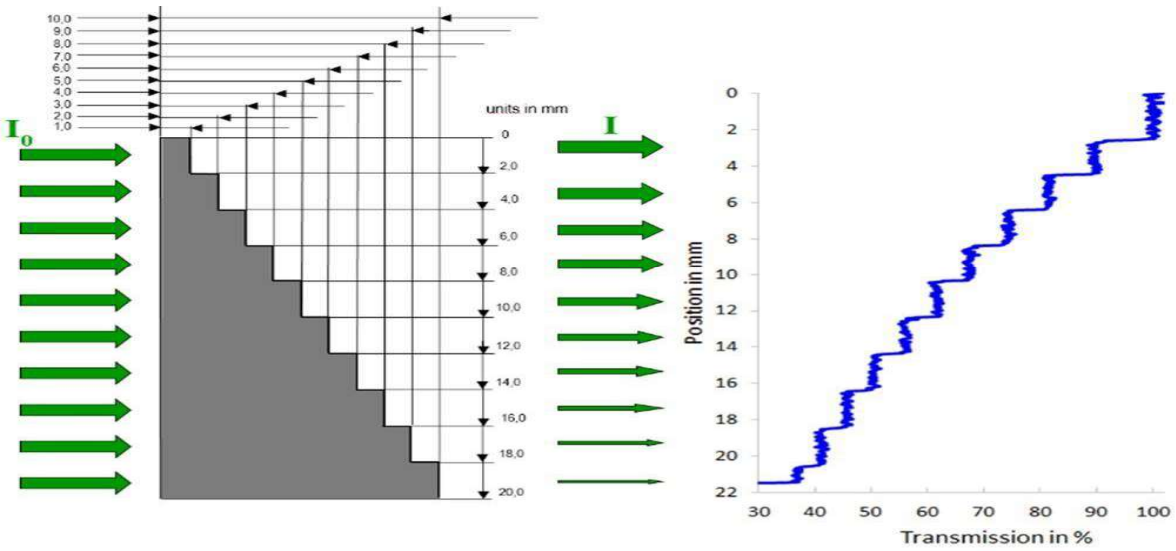

FIGURE 3: Physical high purity graphite standard (left, dimensions in mm indicated) radiated by parallel X-rays of an incident intensity I_0 and recorded X-ray transmission I by a spatial sensitive line sensor (right).

To determine spatial resolution of the sensor system, a commercial bar pattern standard (Funk Reinhold, test pattern type 53) was used, where bars and distance between them become smaller and smaller. Fig. 4 displays recorded change of transmission intensities between tightening bars over the 20 mm long standard (top). From these data the so-called transfer contrast function can be calculated. Obtained contrast values are depicted as points in Fig. 4 (bottom). Intensity differences of 0.1 (contrast) can be resolved by the sensor system. Extrapolation of transfer contrast function (dotted line) to minimum detectable contrast yields a spatial resolution of at least 35 µm.

The full protection security system of LUMiReader X-Ray was certified by PTB – National Metrology Institute of Germany, Braunschweig, and Federal Office for Radiation Protection (BfS) of Germany. The analytical instrument can be used free of risk and with no specific training course of X-ray radiation safety, nor any special operational license to user.

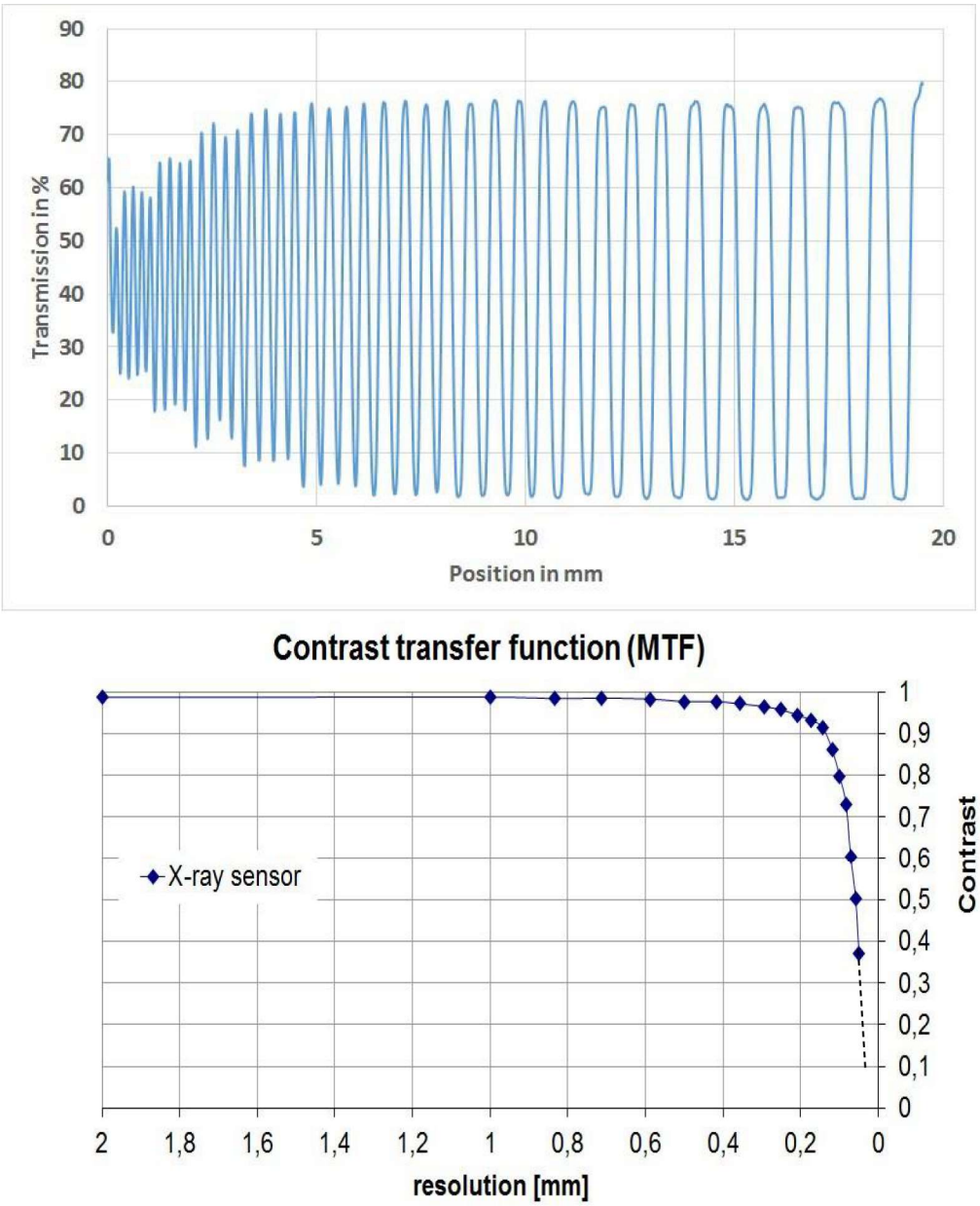

FIGURE 4: Spatial transmission intensity variation for a bar pattern standard (top) and contrast transfer function (bottom) to determine spatial resolution by extrapolation to minimum contrast detection (broken line).

RESULTS AND CONCLUSION

Preliminary tests of LUMiReader X-Ray revealed a broad spectrum of applications for concentrated dispersions, transparent or opaque ones. On the one hand, they reach from evaluation of homogeneity of dispersed phase (e.g., dispersibility, miscibility) to stability characterization (e.g., phase separation, alterations of dispersion state, segregation). On the other hand, concentration profiles within dispersions, filter cakes or sediments may be determined. This allows in situ characterizing consolidation phenomena and packing densities (solidosity) at gravity or at applied external forces. Finally, it should be mentioned that nanoparticles may be detected in transparent dispersions (supernatants) or separated phases in highly opaque dispersions. Due to time limitation, we are going to discuss only three applications in more detail.

3.1. Phase separation at gravity:

Stability of fillers dispersed in an adhesive matrix (3 different formulations) was investigated during 46 days of storage at room temperature. Fig. 5 (left) depicts progressing phase separation. Red profile corresponds to initial situation (about 35 % transmission) after formulation (0d). It shows good homogeneity of dispersed filler particles throughout the entire sample after formulation, which holds also after the first storage day. But phase separation is clearly detectable after 4 days. Filler "free" layer is indicated by the sharp transmission decrease from a transmission > 80 % to the base line (about 35 %), which is typical for zone or monodisperse sedimentation. This interphase progressed until day 46 (dark green profile), but

"clarification" of supernatant is less (only about 70 %) and transmission profile at interphase is less sharp indicating the formation of a concentration gradient over about 2.5 mm. On the other hand, transmission above the bottom decreases due to filler sediment formation. It should be underlined that visual evaluation by naked eye does not allow detecting any phase separation (Fig. 5, photo at the top). Height of supernatant was quantified for the three different formulations by Front Tracking Analysis of SEPView. Results reveal significant differences between the three differently formulated dispersions analysed (Fig. 5, right). separation by naked eye (photo on top). On the right: Comparison of filler separation of three differently formulated adhesive products (quantification by height of supernatant).

A second example of real-time stability analysis is given in Fig. 6 for a multicomponent dispersion – a Molybdenumdisulfide (MoS_2)/Graphite lubricant. As this dispersion is dark black, no visual observation was possible. In contrast, X-ray profiling allows monitoring time dependent phase separation. First measurement (red profile) shows same transmission (attenuation) over the entire sample height indicating same concentration of all components throughout the sample (good dispersion process). During storage phase separation occurs, documented by gradual increase of transmission in the top region and decrease in bottom region, respectively. Final sediment height amounts about 5 mm after 62 days. A closer look on transmission profiles in sediment region reveals sediment structures. Registered attenuation near the bottom of sample cell and the top of the sediment are higher than in middle of sediment. The reason may be different packing (solidosity, volume

concentration) due to local fractionation/segregation of dispersed phases. Different sedimentation and packing may be caused by polydispersity of particles regarding size, shape or materials density. This example proves characterization of phase separation of multicomponent systems (binary suspensions).

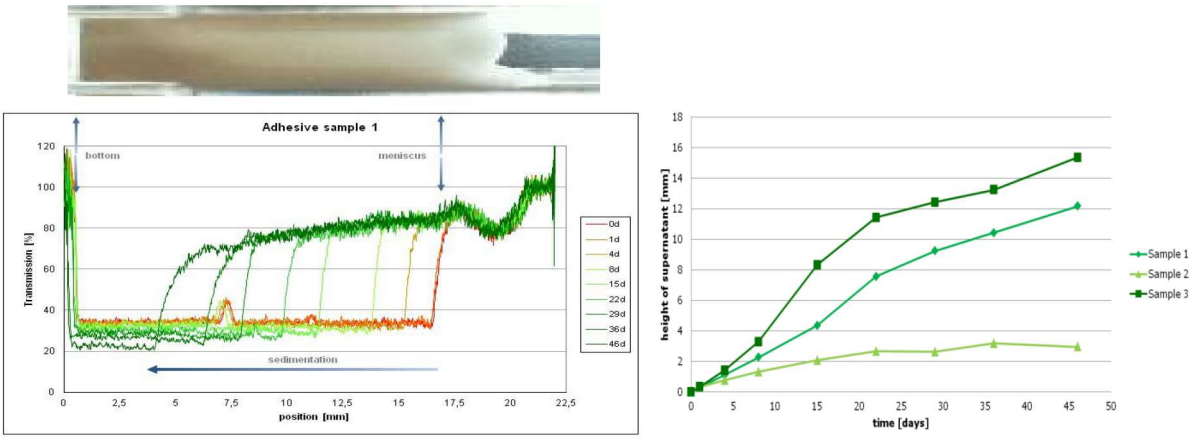

FIGURE 5: Detection of real time phase separation kinetics within a filler containing adhesive dispersion during storage for 46 days (46d) at room temperature (fingerprint, left). Opacity of adhesive matrix does not allow evaluating phase.

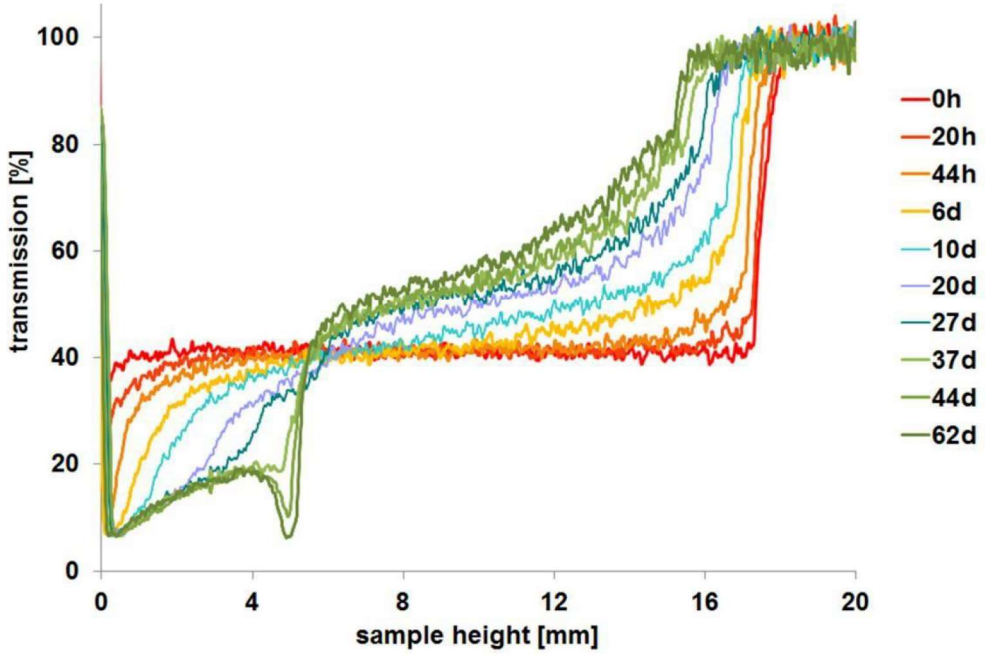

FIGURE 6: Kinetics of transmission changes (time coded by colors) of a Molybdenumdisulfide-Graphite suspensions (MoS_2-Graphite) during storage of 62 days at room temperature.

3.2. Consolidation analysis:

Processing of dispersion based products involves beside gravity settling often centrifugation steps for solid-liquid separation. On the other hand, in case of products exhibiting long-term stability, acceleration procedures, as centrifugation, may be applied [1]. In both cases knowledge of dependency of phase separation behaviour on centrifugal acceleration or centrifugal force, respectively, would be of interest. To this end detailed information may be obtained by combining analytical photocentrifugation and X-ray profiling as the same sample cells may be used in both analysers. General approach would be to apply first e.g., excess pressure by centrifugation and at given time intervals samples are removed from rotor and Xray profiling performed. It was already shown that equilibrium sediment heights for constant (static, cp. Fig. 7) or stepwise (dynamic) increase of centrifugal acceleration determined by both techniques

reveal the same sediment heights [6, 7]. In other words, average packing density or solidosity are the same. As proposed by Buscall [8] and recently detailed analysed [9, 10], final packing density after centrifugal separation exhibits information regarding, e.g., mechanical properties of sediments (strength of particle networks) of flocculated mineral slurry and biological sludge. Determined compressional yield stress allows predicting performance of dewatering of industrial processes as gravity settling, centrifugal and filtration.

As already discussed in chapter 3.1. (e.g., Fig. 6), concentration within sediment may change with position due to segregation of different kinds of particles. In a subsequent paper we report on this conference about separation and segregation behaviour of model paper dispersions made of paper constituents cellulose and inorganic kaolin powder (details this proceedings, [11]). Local packing concentration also depends on particle-particle interaction. As shown in Fig. 8, in contrast to stable suspensions, flocculated dispersions consolidate and concentration gradients are building up for a series of consecutive experiments performed at different constant (static) rpm or excess pressures, respectively [6]. This may be the reason that in case of dynamic increase of excess pressure local sediment structure and particle volume concentration (solidosity) depend on course of centrifugal acceleration during sediment formation and not only on local excess pressure value as demonstrated by Loginov et al. [7] for kaolin suspensions by means of X-ray concentration profiling.

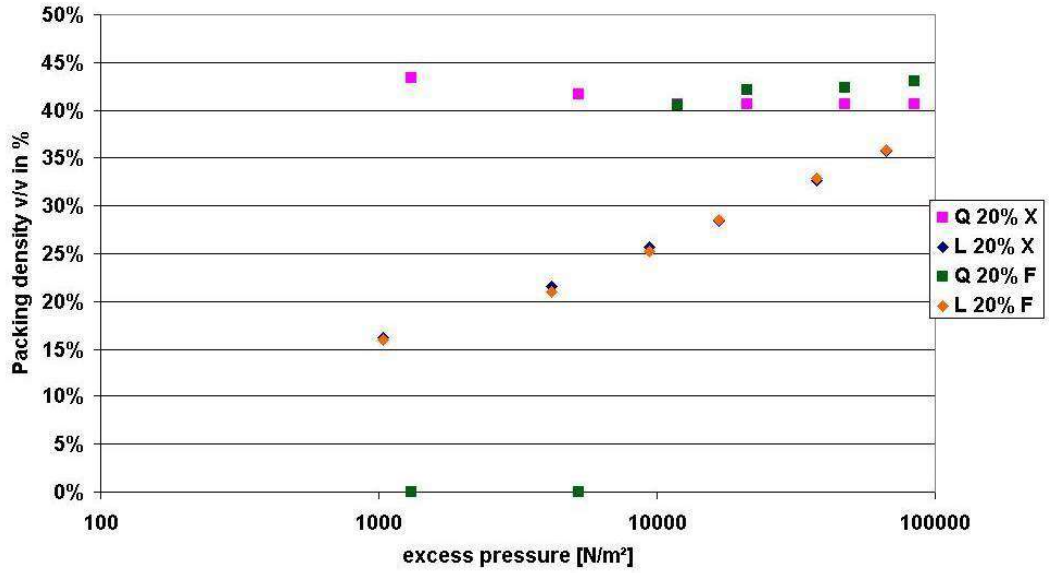

FIGURE. 7: Sediment packing density after phase separation of stable quartz (Q) and flocculated limestone (L) suspensions (initial volume concentration amounts 20 % in both samples) in dependence on excess pressure (equilibrium data) obtained by optical (F) and X-ray (X) concentration profiling. Note 1: Optical data were obtained in situ and for X-ray analysis samples after centrifugation were carefully placed into the X-ray LUMiReader. Note 2: Sediment thickness of quartz for excess pressures smaller 10,000 N/m² can not be determined due to opacity with light transmission (green squares).

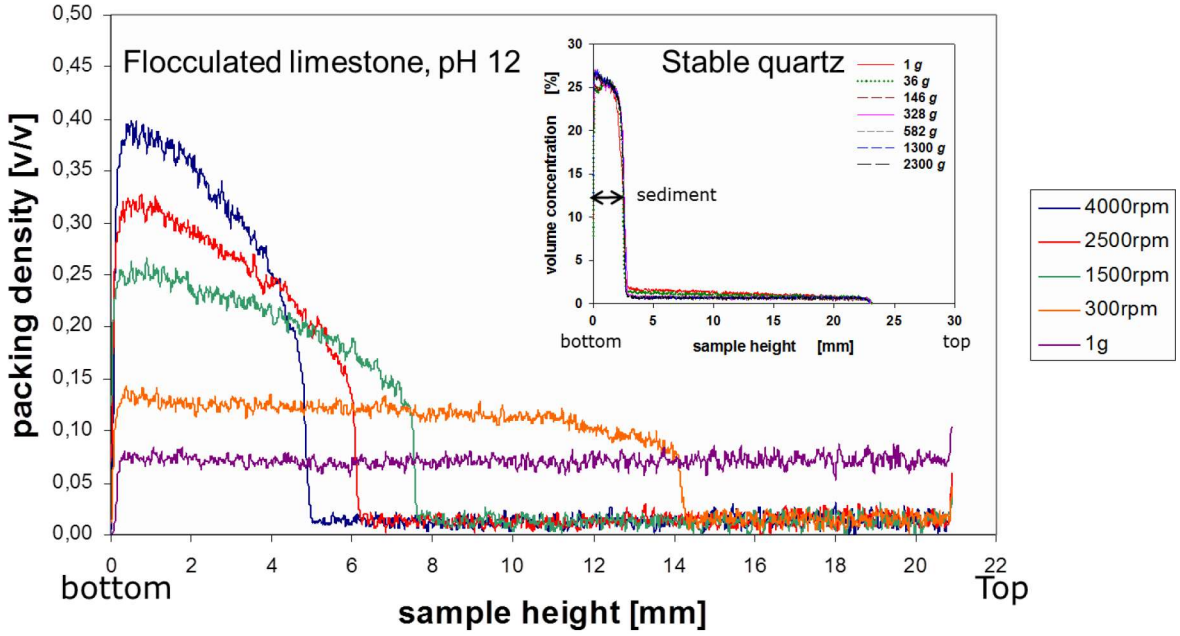

FIGURE 8: Comparison of consolidation behaviour of stable (quartz) and flocculated (lime stone) suspensions obtained at different centrifugal accelerations (rpm), respectively excess pressures. The 1 *g* concentration profile was measured before centrifugation.

Sediment structure depends also on type of flocculent used for solid-liquid separation. In Fig. 9 we show typical results for waste water clarification by nanoclay mineral flocculants [12]. Plate-like nanoparticles (Hektorite) formed flocks separate into very compact sediments. Sediment height is about 1 mm independent on relative centrifugal acceleration (RCA) and maximum attenuation coefficient (measure for sediment density) amounts at RCA = 50 about 3.5 cm^{-1} and increases to 6.5 cm^{-1} at RCA = 1800. In contrast, sediments of waste flocks built by needle-like nanoparticles (Palygorskite) exhibit very thick sediments which consolidate from about 8 mm (RCA = 50) to 3 mm at RCA = 1800. On the other hand, sediment packing is much less pronounced and maximum attenuation coefficient reaches even for RCA = 1800 only about about 3 cm^{-1}.

3.3. Detection of nanoparticles:

Concentrated suspensions are normally turbid or opaque. But in case of nanoparticles with a size from nanometers up to tens of nanometers, suspensions even for very high volume concentrations are transparent, as due to Rayleigh law these very small particles does not scatter enough visible light. In contrast, X-ray attenuation takes place even for real solutions (e.g. sodium chloride) as it does not depend on particle size. Fig. 10 (top) shows visual appearance of nanoparticle solutions (Koestrosol K1530, 15 nm) with increasing volume concentration. The letter “U” behind the sample cells can be seen clearly. At bottom mean values of measured X-ray transmissions are displayed, which reads 79.05 % for water and decreases with increasing Koestrosol concentration to 61.04 % in case of 30 v/v%. Maximum standard deviation was 0.13 % in case of pure water.

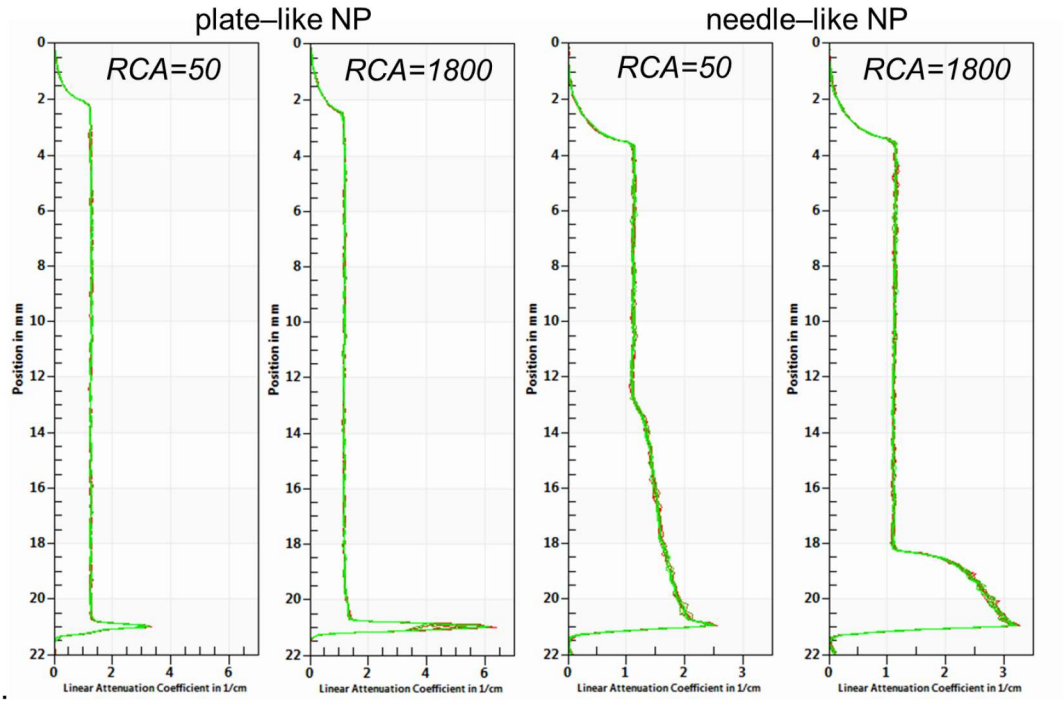

FIGURE 9: Comparison of waste water cleaning by differently shaped mineral clay nanoparticles. X-ray attenuation profiles were obtained after flocculation of waste and solid-liquid separation by analytical centrifugation (LUMiSizer) at different RCA. Note the different scaling of attenuation aches.

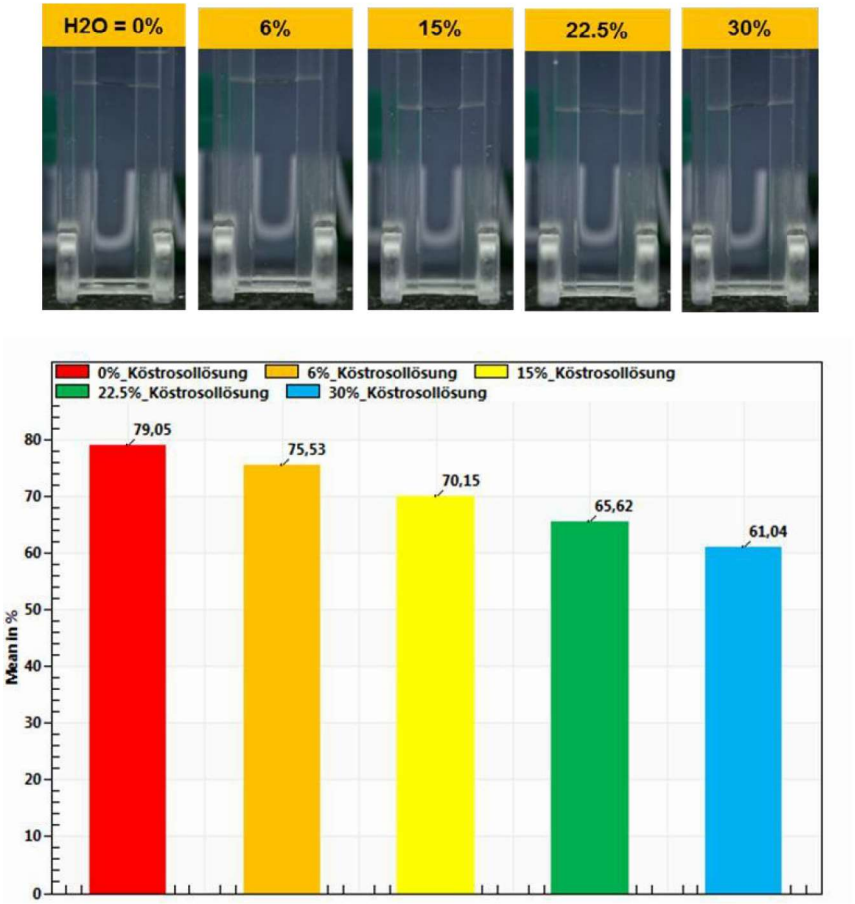

FIGURE 10: Photographs of nanoparticle suspensions up to 30 v/v% (top, right) and corresponding mean values of X-ray transmission over the entire sample height.

Detection of nanoparticles by LUMiReader X-Ray opens interesting applications. It allows identifying nanoparticles in complex dispersions. For demonstration microsized quartz (x_{median} = 2 µm,) and nanozised Koestrosol (x = 15 nm) was dispersed in water. Final volume concentration amounts 10 w/w% quartz and 30 w/w% Koestrosol. Dispersion was centrifuged by LUMiSizer (RCF = 2300, t = 10 min, 2 mm PC cells). As photograph at top of Fig. 11 demonstrate, the dispersion before segregation is completely opaque, as expected. After 10 minutes of centrifugation a separation took place. A clear supernatant and sediment are visible by naked eye. Supernatant appearance (top, right) does not differ from continues phase – pure water (top, left). Corresponding X-ray profiling of these three samples is also shown in Fig. 11 (bottom). As to expect, water exhibits a transmission of about 80 % (green line). Dispersion before centrifugation attenuates much stronger and average transmission amounts of about 52 % (red) over the entire sample cell. After centrifugation a sediment of about 2 mm thickness, visible also by naked eye, is clearly demonstrated (blue).

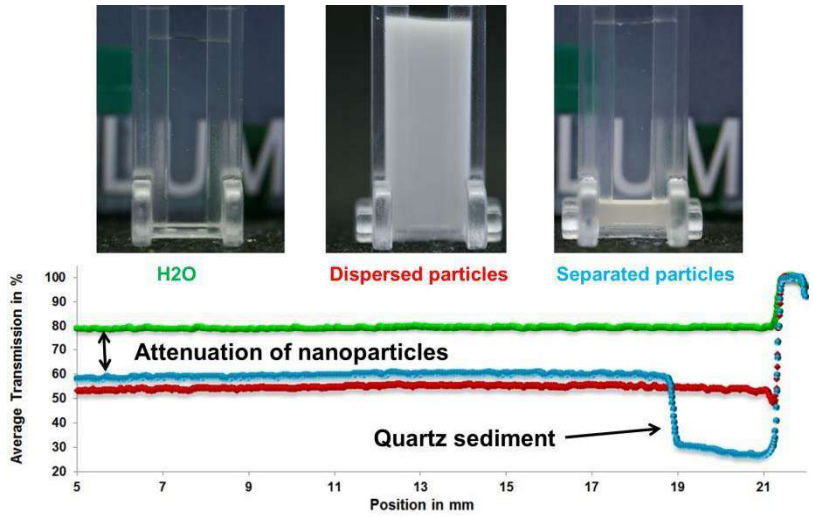

FIGURE 11: Visual appearance (top) and X-ray profiling (bottom) of pure water and a mixture of microsized quartz (x_{median} = 2 µm,) and nanozised Koestrosol (x = 15 nm) dispersed in water before and after centrifugal separation at RCF = 2300 for 10 min.

Interestingly, there is a difference in transmission between pure water and the clear supernatant after centrifugation. The lower transmitted intensity is due to attenuation of dispersed nanoparticles, not separated within 10 min centrifugation. The about 20 % lower transmission compared to pure water corresponds well with the data of Fig.10. Nanoparticles, as Zincoxide in sun cream emulsions, may be also detected by X-ray profiling. To demonstrate this, a product from the super market was centrifuged for a longer time as for the application above and inserted into the LUMiReader X-Ray for nanoparticle detection. As shown in Fig. 12, the emulsion does not exhibit additional attenuation (expressed as extinction) compared to water due to low atomic numbers of its constituents. But at the bottom of sample cell a distinct thin layer of higher attenuation was clearly to observe due to segregated Zincoxide. Based on the above findings a promising approach may be worked out to detect nanoparticles within complex dispersions.

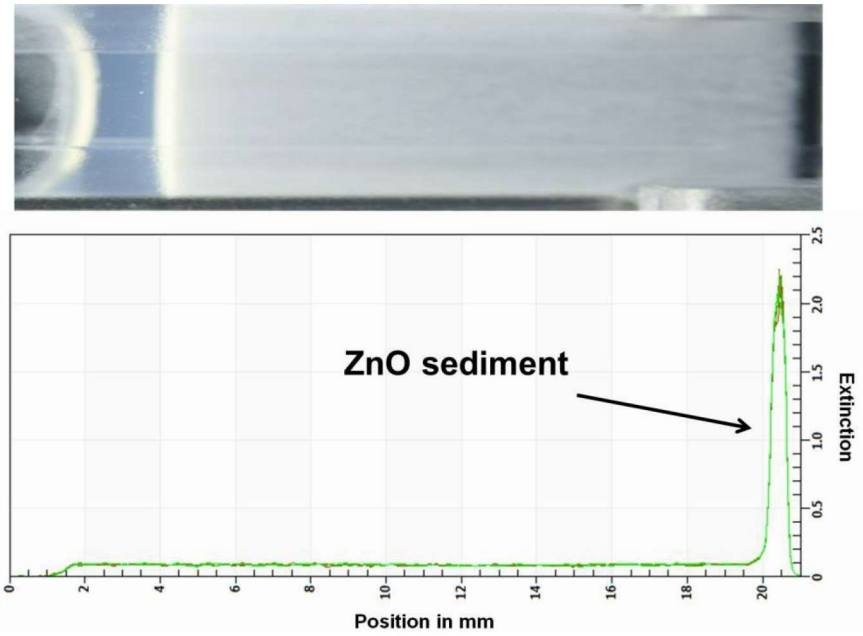

FIGURE 12: Pigment (ZnO) segregation detected within opaque sun protection cream after centrifugation for 120 min at RCF = 2300 (LUMiSizer) and attenuation profiling (LUMiReader X-Ray). Top: Photo after centrifugation.

CONCLUSION

LUMiReader® X-Ray based on STEP-Technology® (Space and Time resolved Extinction Profiles) extended X-ray intensity profiling allows qualitative and quantitative characterization of dispersion state of entire sample even in case of highly concentrated formulations and products independent on its optical properties – transparent or opaque. Experimental analysis is performed in situ (contact-free) with nascent, undiluted samples. Quantification and concentration determination is eased, compared to any optical method, as the transmitted signal does only depend on atomic number of materials and its mass concentration but not on size or shape of dispersed particles. Furthermore, concentration profiles in dispersions or local packing densities (solidosity) of sediments as well as their alteration due to time or applied excess pressure changes can be studied regarding particle-particle inter-action or mechanical sediment properties like compressional yield stress. Importantly, for binary suspensions (mixtures of different dispersed materials), segregation can be evaluated based on different X-ray absorption of dispersed particles. Nanoparticles may be detected in transparent supernatants as well as after phase separation in highly opaque cosmetic matrixes.

ACKNOWLEDMENT

Authors gratefully acknowledge Institut fuer angewandte Photonik (Inst. of Appl. Photonics e.V., IAP e.V.) Berlin for his continues support.

REFERENCES

[1] ISO/TR 13097: 2013. Technical Report. Guidelines for the characterization of dispersion stability.

[2] D. Lerche and T. Sobisch, Direct and Accelerated Characterization of Formulation Stability. J. Dispersion Sci. and Technol. 2011, 32 (2011) 1799–1811.
[3] D. Lerche and T. Sobisch, Evaluation of particle interactions by in situ visualization of separation behaviour. Colloids and Surfaces A: Physico-chemical and Engineering Aspects 440 (2014) 122 – 130.
[4] T. Sobisch, F. Emmerling, M. Girod, M. Menzel, D. Lerche, Advantages of dual wavelength detection for size determination of nanoparticles with analytical centrifugation. Dispersion Letters 4 (2013) 9 – 11.
[5] B. Luigjes, D.M.E. Thies-Weesie, A.P. Philipse, A. and B.H. Erne, Sedimentation Equilibria of Ferrofluids: I. Analytical Centrifugation in Ultrathin Glass Capillaries. J. Phys. Condens. Matter 24 (2012) 245103.
[6] D. Lerche, Keynote Lecture: Sedimentation and consolidation behavior of stable and flocculatedsuspensions. Direct in-situ visualization and analysis. Proceedings of Int. Conference and Exhibition for Filtration and Separation Technology, Wiesbaden, Germany; Oct. 22nd – 24th, 2013.
[7] M. Loginov, D. Kavianpour, A. Zierau, J. I. Martinez Sánchez, N. Lebovka, T. Sobisch, D. Lerche, E. Vorobiev, Determination of pressure dependence of particle volume fraction: combination of centrifugal methods with X-ray analysis of local sediment structure. Proc. 2nd European Conf. on Fluid-Particle Separation, Lyon, Oct. 14th – 17th, 2014.
[8] P. Buscall R. L.R. White, The consolidation of concentrated suspensions. J. Chem. Soc., Faraday Trans. 1 83 (1987) 873-891.
[9] S.P. Usher, L.J. Studer, R.C. Wall, P.J. Scales, The characterization of dewaterability of equilibrium and transient centrifugation test data. Chem. Eng. Si. 93 (2013) 277-291.
[10] M. Loginov, E. Vorobiev, N. Lebovka, O. Laure, Compression-permeability characteristics of mineral sediments evaluated with analytical photocentrifuge. Chem. Eng. Sci. 2011, doi: 10.1016/j.ces.2010.12.041.
[11] T. Sobisch, S. Horvat, D. Kavianpour, A. Zierau, D.Lerche, Characterization of the separation and segregation behaviour of model paper dispersions. This proceedings. [12] G. Rytwo et al.: The use of an X-ray dispersion analyzer to study sedimentation patterns: clay minerals as an example. To be published.